


**Please cite the Published Version**

Manning, A, Qian, L  and Erfani, R (2024) CFD modelling of velocity fields around a fume cupboard: Evaluating static and dynamic meshes with experimental measurements. *European Journal of Mechanics - B/Fluids*, 105. pp. 238-246. ISSN 0997-7546

**DOI:** <https://doi.org/10.1016/j.euromechflu.2024.01.014>

**Publisher:** Elsevier BV

**Version:** Published Version

**Downloaded from:** <https://e-space.mmu.ac.uk/633840/>

**Usage rights:**  [Creative Commons: Attribution 4.0](https://creativecommons.org/licenses/by/4.0/)

**Additional Information:** This is an Open Access article published in *European Journal of Mechanics - B/Fluids*, by Elsevier.

**Data Access Statement:** The authors do not have permission to share data.

**Enquiries:**

If you have questions about this document, contact [openresearch@mmu.ac.uk](mailto:openresearch@mmu.ac.uk). Please include the URL of the record in e-space. If you believe that your, or a third party's rights have been compromised through this document please see our Take Down policy (available from <https://www.mmu.ac.uk/library/using-the-library/policies-and-guidelines>)



Contents lists available at ScienceDirect

## European Journal of Mechanics / B Fluids

journal homepage: [www.elsevier.com/locate/ejmflu](http://www.elsevier.com/locate/ejmflu)

# CFD modelling of velocity fields around a fume cupboard: Evaluating static and dynamic meshes with experimental measurements

A. Manning<sup>a,1</sup>, L. Qian<sup>a,2</sup>, R. Erfani<sup>b,c,\*</sup>,<sup>3</sup>

<sup>a</sup> Manchester Metropolitan University, Department of Computing and Mathematics, John Dalton Building, Chester Street, Manchester M1 5GD, United Kingdom

<sup>b</sup> Manchester Metropolitan University, Department of Mechanical Engineering, John Dalton Building, Chester Street, Manchester M1 5GD, United Kingdom

<sup>c</sup> University College London, Department of Civil, Environmental and Geomatic Engineering, Gower Street, London WC1E 6BT, United Kingdom

## ARTICLE INFO

## Keywords:

Fume cupboard  
Fume cupboard testing  
Overset meshing  
Dynamic meshing  
CFD

## ABSTRACT

This paper presents a comparison of experimental and numerical modelling results of the velocity field around a fume cupboard with a static and a dynamic mesh. During fume cupboard testing, components are required to move which mimic typical operating conditions, the amount of tracer gas released is then measured. This tracer gas is harmful to the environment and so an alternative is required. Advanced Computational Fluid Dynamics (CFD) techniques, such as dynamic meshing, have been utilised to replicate aspects of the current tests. The fume cupboard was tested in normal operating conditions and under the influence of a board inducing a wake close to the fume cupboard entrance. The velocity fields have been compared and show a reasonable level of accuracy with a percentage difference between experimental and simulated results of around 5% using both a static and a dynamic domain. This is an improvement on the 15–20% accuracy for detecting concentration of tracer gas using previous experimental methods. The aim of this work is to satisfy the scientific community and fume cupboard operators that CFD is sufficiently accurate to assess fume cupboard performance under real world scenarios.

## 1. Introduction

Fume cupboards are widely used in laboratories, from universities to pharmaceutical companies to protect users from hazardous gases, splashes and suspended particles. Before installation, the fume cupboards should be tested in a quiescent environment above 20 °C [1], then on site during commissioning and periodically thereafter [2]. Each of these three test points have varying levels of detail, the most stringent of which is the type test, conducted in the ideal conditions to prove the fume cupboard adequately contains gas.

The British Standard testing method uses a tracer gas made up of 90% nitrogen by volume and 10% sulphur hexafluoride (SF<sub>6</sub>). SF<sub>6</sub> is used because it can be detected at concentrations as low as 6 ppb [3] with a resolution of 1.5 ppb, meaning even small amounts of gas can be detected leaving the fume cupboards. This low detection level means

that the injection rate of the gas can be low, so the influence of the gas injection on the fume cupboard performance is negligible. SF<sub>6</sub> has a global warming potential of 22,800 at 25 °C [4], meaning a single type test [1] releases the equivalent of around 3100 kg of CO<sub>2</sub>. This is not in-keeping with the global drive towards sustainability and the government's net zero target [5], hence, finding a new approach to test the fume cupboards is crucial.

The British and European standard for fume cupboard type testing [1] is made up of four tests. The tests measure the concentration of tracer gas in front of the fume cupboard, or in the extraction duct. Two of the tests use a static domain, two use a dynamic domain. Here, a static domain is one where the walls and boundaries remain stationary and a dynamic domain is one where some of the walls move relative to one another. In order for Computational Fluid Dynamics (CFD) to become a viable alternative for fume cupboard testing, it must be proven to

*Abbreviations:* CFD, Computational fluid dynamics; CFL, Courant-friedrichs-lewy; MAPE, Mean absolute percentage error; RANS, Reynolds averaged navier stokes.

\* Corresponding author at: Manchester Metropolitan University, Department of Mechanical Engineering, John Dalton Building, Chester Street, Manchester M1 5GD, United Kingdom.

*E-mail address:* [r.erfani@mmu.ac.uk](mailto:r.erfani@mmu.ac.uk) (R. Erfani).

<sup>1</sup> 0000-0002-2468-6989

<sup>2</sup> 0000-0002-9716-2342

<sup>3</sup> 0000-0002-4178-2542

<sup>1</sup> Based on a fume cupboard with a sash width of 1700 mm.

<https://doi.org/10.1016/j.euomechflu.2024.01.014>

Received 4 July 2023; Received in revised form 21 January 2024; Accepted 23 January 2024

Available online 31 January 2024

0997-7546/© 2024 The Author(s). Published by Elsevier Masson SAS. This is an open access article under the CC BY license (<http://creativecommons.org/licenses/by/4.0/>).

produce accurate results of the static and dynamic tests.

Previous work has presented alternative test methods which have been compared to determine which factors are most important to fume cupboard performance. Ahn et al. [6] summarised that the presence of a manikin in front of the fume cupboard, distance of the injector to the sash and sash opening height were key to fume cupboard performance in the tests.

In other work, CFD has been seen as a possible alternative to tracer gas testing for over 20 years [7]. The same team then tried to develop a testing strategy for fume cupboards [8]. Unfortunately, dynamic meshing was not possible at the time, making it impossible to simulate the real world scenarios with moving parts as laid out by the current standard [1]. This is an area the present work has considered.

Later, fume cupboard design was improved through the use of CFD [9], two designs were compared, showing a favourable improvement in the velocity fields between the designs. The improved velocity field would have a beneficial impact on containment and therefore safety. Further work.

was conducted to assess and model the impact of a push-pull fume cupboard [10] and found that the push-pull fume cupboard performed better under static conditions. Together, [9,10] showed that CFD has the potential to simulate fume cupboard and help the design process, although more work is required to replace testing. The aim to improve fume cupboard performance using CFD has continued recently.

[11] where experimental measurements were compared to simulated values over three static domains.

The present work aims to create a suitable CFD model for flow fields around a fume cupboard, specifically when components are moving. To the best of our knowledge, the application of moving meshes in CFD on fume cupboards has not been reported, however, this capability is vital for CFD. In this study, we use dynamic meshes and show that CFD can become a viable alternative to the type test method in the near future.

The aim will be achieved through applying advanced CFD and meshing techniques for modelling flow around a fume cupboard under both static and dynamic conditions. For the case of a static domain, the velocity will be examined in detail at the sash opening and compared to the experimental results. For the dynamic domain, we consider a point in the centre of the fume cupboard when a board, which is used in BS EN 14175-3 [1], passes the fume cupboard. To model the large amplitude rectilinear motion of the moving structure, the overset grid method will be applied and the velocity results from experiment will be compared to those from the simulations. The flow field around the moving board and its effects on the face velocity of the fume cupboard will be discussed.

For the study to show CFD as a viable alternative, it must be as accurate, or better than current measurement equipment. The percentage error of the SF<sub>6</sub> measuring equipment varies based on the gas detector but is typically around 15–25% for the low concentrations. Therefore to achieve the project aim, CFD results should produce a better level of accuracy than is available using tracer gas methods.

The paper is organised as follows. In Section 2, the experimental measurements will be presented including details on experimental equipment. Section 3 will discuss the numerical modelling and CFD approaches utilised. The results will then be presented and discussed in Section 4. During Sections 2–4, each section is split into two, one looking at a static domain, and one looking at a dynamic domain.

## 2. Experimental testing

Containment of gas within a fume cupboard is largely controlled by the velocity profile around the face of the fume cupboard [7], the average of this velocity field is known as the face velocity and is a key design criteria. It is defined as the average velocity of air entering the fume cupboard across the sash entrance. The sash entrance is a plane defined along the centre of the sash in the direction of its vertical movement. It extends across the width of the sash opening, then from the sash handle down to the aerofoil (if fitted) or the worktop otherwise.

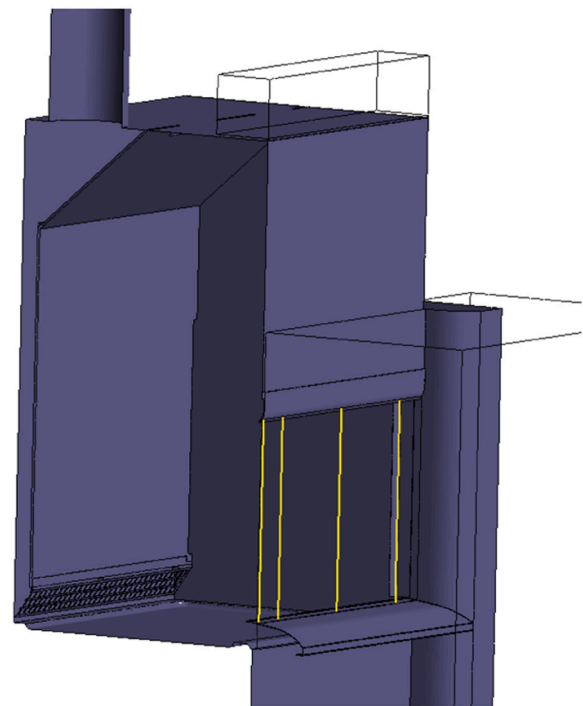


Fig. 1. Location of lines for comparison of the static domain velocity field, Lines 1–4 are identified from left to right.

The yellow lines in 1 are in the sash opening.

A low face velocity, or poorly designed air distribution at the face of the fume cupboard may cause gas to be emitted. Because the face velocity is a very important parameter in designing fume cupboards, in this work, we focus on analysing it and compare its value obtained using CFD with those measured in experiment.

The face velocity of most fume cupboards is often between 0.3 m/s and 0.5 m/s with most tending towards the higher value due to better containment. When considering the British Standard [1], the injection velocity during the inner plane test is around 0.02 m/s at a distance of 150 mm inside the fume cupboard. When looking at the outer plane test and the robustness test, the injection rate falls even lower and is 200 mm inside the cupboard from the face of the fume cupboard. This means the injection of SF<sub>6</sub> has very little impact on the velocity field at the sash opening.

Due to the low impact on face velocity, the injectors can be neglected from experimental measurements. This has the additional advantage that the flow around the fume cupboard is now a single phase, which simplifies the air flow in CFD simulations.

Tests were devised to measure the velocity at the sash for two domain types, static and dynamic. The velocity was measured using a calibrated set of three TSI 8445 [12] anemometers. Data was recorded at a rate of 1 Hz using a data logger connected to a PC. An 1800 mm wide Radius Profile fume cupboard [13] was provided for the purposes of testing by Clean Air Ltd. In all tests, the probes were clamped in position ensuring they are fixed. In addition, the clamping arrangement allowed controlled movement along a single orthogonal axis. During all tests, the sash open working height was 500 mm and the extraction rate was varied to give two average face velocities of 0.5 m/s and 0.3 m/s.

### 2.1. Static domain

A series of four vertical lines were considered at the face of the fume cupboard; these are shown in Fig. 1. The velocity was measured along these lines as the height in the sash opening varied.

The first vertical line was placed in the centre of the fume cupboard.





Fig. 2. Experiment setup of static domain measurements.

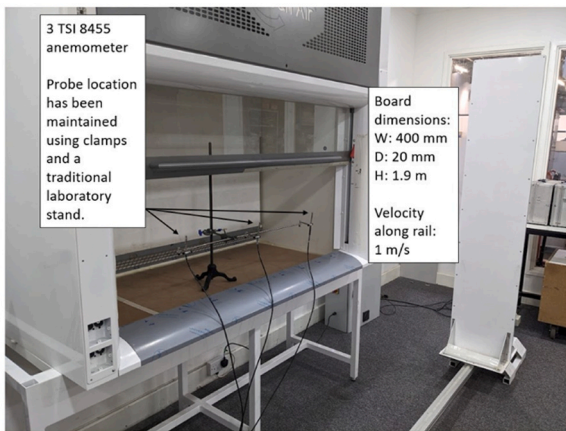


Fig. 3. Experimental setup of dynamic domain measurements.

Line 2 was placed 100 mm to the right of Line 1, and Line 4 was placed 100 mm to the left of the right hand boundary. Line 3 was placed half way between Line 1 and the right hand side of the fume cupboards face. Along each vertical line, 11 equally spaced measurement locations were selected. These locations were at 50 mm intervals although a 5 mm offset was required at the top and the bottom of the sash opening due to the anemometers shielding.

The velocity was measured at each location for a total of 30 s at a rate of 1 Hz. Since there was no motion, and the fume cupboard was operating in a steady state, a faster data rate was not required. A TSI 84455 anemometer was connected to a data logger and the data rate was set.

Fig. 2 shows the experimental arrangement of the static domain measurements. The anemometer probe was placed inside the fume cupboard, in Fig. 2 the probe is placed in the centre of Line 1. Simultaneously, the data logger was connected to a venturi flow meter, meaning the volumetric flow rate is measured at the same time as the face velocity. Wherever possible, the measurement equipment was outside the fume cupboard to minimise the influence of the equipment on the air flow.

## 2.2. Dynamic domain

One of the type tests in the British Standard is the robustness test. During this test, a board passes in front of the fume cupboard at a rate of 1 m/s passing parallel to the fume cupboard face at a distance of 400 mm, as shown by Fig. 3. The board moves along a rail to ensure the motion is linear and parallel to the face of the fume cupboard. The movement is driven by a motor ensuring a constant velocity. As the

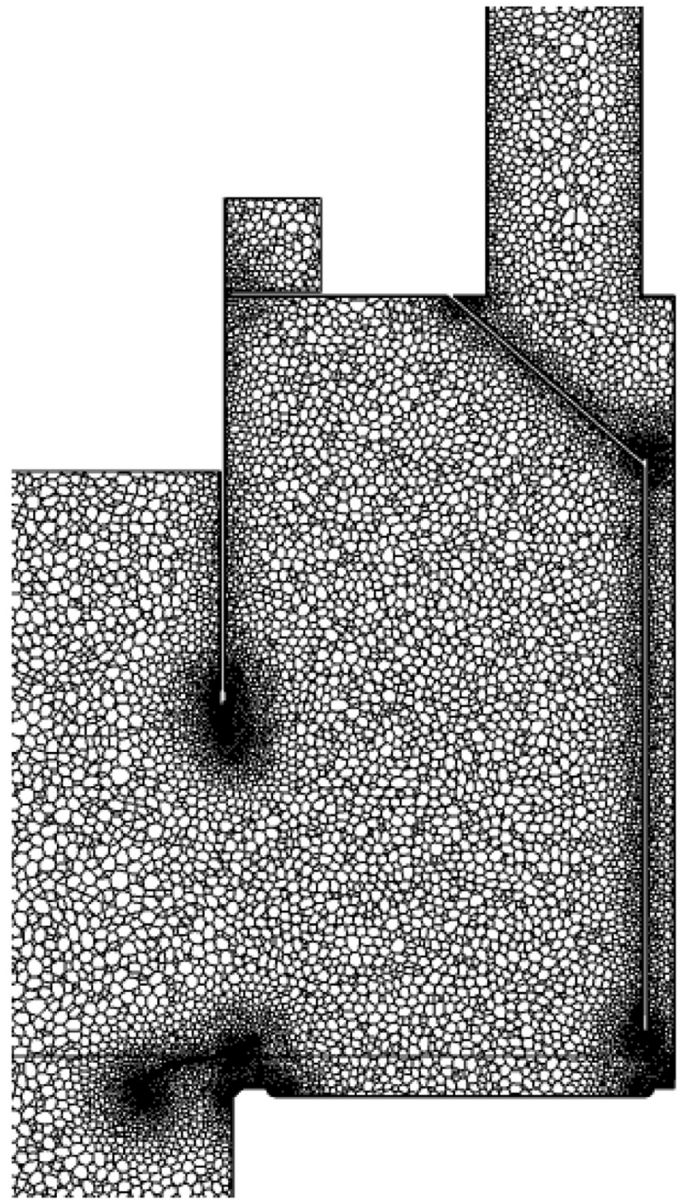


Fig. 4. Polyhedra mesh used for the static domain simulation.

board passes, the bow wave and wake both influence the face velocity, and therefore containment.

To measure the impact of the boards induced velocity field, an anemometer was placed 100 mm from either side of the sash entrance and one in the centre. All probes were in line with the sash plane and in the centre of the sash height, at 250 mm above the aerofoil. The velocity of air entering the fume cupboard was measured at a rate of 100 Hz and reported at each location whilst the board passed by. The measurements were conducted 5 times, then the maximum, minimum and average were found.

The volumetric flow rate of the fume cupboard was also measured through a venturi flow meter placed in the extraction duct. This was used to define the boundary conditions described in Section 3.2.

## 3. Numerical simulations

The static and dynamic simulations were conducted using StarCCM+ utilising a transient Reynolds Averaged Navier Stokes (RANS) solver [14].

A maximum Courant-Friedrichs-Lewy (CFL) number of 0.5 was



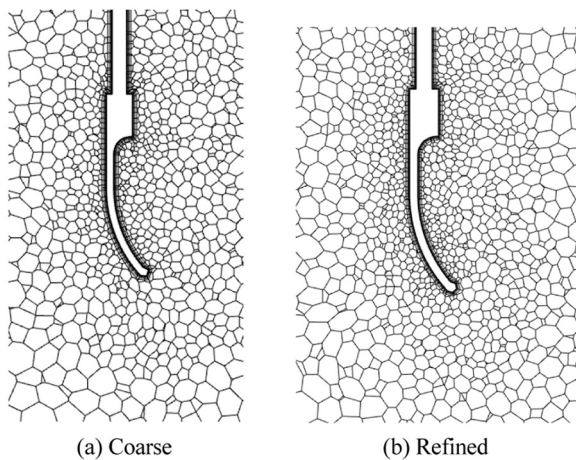


Fig. 5. A comparison of the coarse and refined meshes.

achieved at the face of the fume cupboard. Around the rest of the domain this fell to around 0.03.

The pressure and velocity were coupled using a second order SIMPLEC [15] approach. The convergence criteria for the continuity and the momentum equation was set as 0.001. A second order method was also used throughout for temporal discretisation.

All walls were considered as no-slip boundaries without additional wall functions. The static domain test was simulated using a geometry representing half of a fume cupboard, since the fume cupboard is symmetrical around the centre plane. The symmetry assumption was wasted and proven, as shown later. This assumption was not possible with the dynamic domain as the board motion creates asymmetrical air flow, meaning the full domain has to be simulated. The simulation was verified against timestep, mesh size and symmetry plane independence.

For the purpose of this paper, the static test and dynamic test refer to the walls within the simulation. Therefore, the static test has no moving boundaries and the dynamic test does have moving boundaries which influence the air movement.

### 3.1. Static domain

In the static simulations the mass flow rates of 0.147 kg/s and 0.245 kg/s were defined at the outlet for the nominal 0.3 m/s and the 0.5 m/s case respectively. These values were half of those measured using a venturi during the experiments, described in Section 2.1, accounting for the symmetrical domain. A zero gradient pressure inlet was applied to the inlet boundaries.

The simulation was run for 15 s, which was sufficient to generate a steady flow field. Results from the simulations based on both laminar flow assumption and various turbulence models, such as  $k-\epsilon$  [16] or  $k-\omega$  [15], were compared, but the use of turbulence model was found to have a negligible impact on the face velocity. Therefore, the  $k-\epsilon$  model was used throughout the current work, this produced an accurate model of the flow given the Reynolds number which was between 10,000 and 16,000 at the sash opening. A polyhedral mesh was created which allows for detailed curvature to be accurately modelled with the centre of the domain being a structured mesh. A polyhedral mesh generates small prismatic cells at the boundaries and larger cells towards the middle of the domain up to a prescribed size or ratio. This is shown in Fig. 4. The baseline mesh contained 1.99 M cells and had a maximum cell size of 20 mm, with refined regions having a refinement down to a 2 mm cell size. A mesh refinement trial was conducted and by adding 50% more cells uniformly across the domain. This is shown in Fig. 5.

The face velocity along Lines 1–4 showed little difference in the velocity vectors. In addition to mesh refinement trials, the impact of timestep was also considered, and the results showed no deviation when

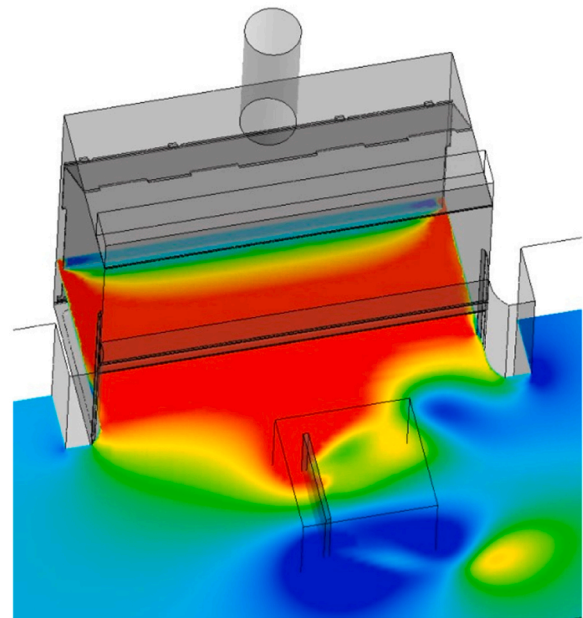


Fig. 6. Overset domain placed inside the background domain of the fume cupboard.

the timestep was halved.

### 3.2. Dynamic domain

The board movement was simulated using an overset meshing approach [17] which considers the domain as two overlapping regions; a background region and a component region enclosed within the background region.

Fig. 6 shows the board within its own domain as outlined by the black lines. This component region is placed inside the same computational space as the background region which represents the fume cupboard.

In the simulation, where the background and component meshes overlap, the numerical values from the background mesh are interpolated to generate the values within the overset mesh. This technique allows for a refined mesh around the component within the coarser background mesh. This method has been used successfully [18] to model fluid motion with moving boundaries in the aeronautical sector. This approach has also been used extensively to model more complex phenomena than a single phase air flow all with a good level of accuracy. Work was conducted looking at the oscillating motion of a submerged sphere in the context of wave energy converters [19], and for the use of floating wave energy converters [20–22]. Later, the same dynamic meshing technique was utilised to model floating wind turbines [23,24].

The overset approach was chosen instead of a dynamic remeshing approach for several reasons. Firstly, the motion of the board was very simple, meaning it could readily be achieved using the overset approach. The board domain could easily be placed within the fume cupboard domain and could move at a fixed velocity for a short period of time, without coming into contact with any walls. This means the motion is simple to describe using the overset method.

The velocity field induced by the board is complex and so the mesh required to model the flow must have a high quality. This is readily achieved using the overset approach because the mesh can have a high quality around the board and only the boundary cells at the interface of the overset mesh will change. Using a remeshing approach, it is possible for cells to become highly skewed which adversely affects the cell quality and may cause inaccuracies in the simulation.

It was found that, in this context, overset method was faster than

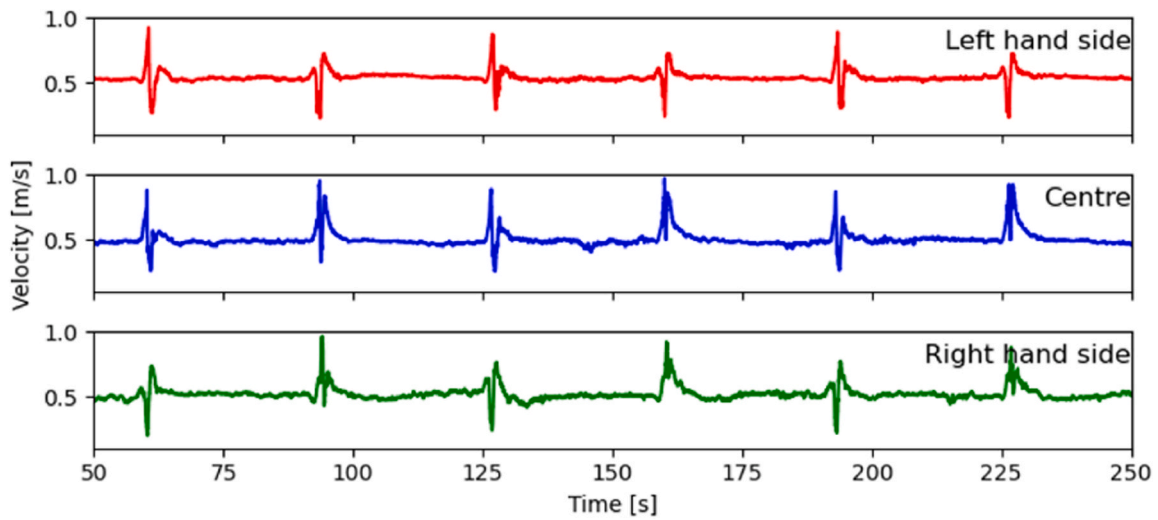


Fig. 7. Cyc c nature of ve oc ty ie d n the robustness test.

remeshing, both for pre-processing and calculation [25–27]. Regarding pre-processing time, the mesh around the board can be made once with a high quality mesh and then imposed into the new fume cupboard as part of the testing simulations. This means a single mesh file can be made for multiple tests. However, a remeshing domain (one which remeshes a region during the simulation based on movement or cell properties) will likely be made in a single mesh file, meaning a new complex mesh will be needed for every fume cupboard.

Additionally, the calculation time of overset meshing is faster than remeshing [25]. This is because the remeshing algorithm will have to make a new mesh every timestep during the boards motion. Comparatively, the overset approach identifies the boundary cells and only those need to be remeshed. The remeshing can be optimised by splitting the domain and only remeshing the area in the path of the board, although it was found the simulation was still slower than the overset method.

For this project, the overset meshing approach offers better scalability with fume cupboard size without having a noticeable impact on simulation time. As the fume cupboard gets bigger, remeshing approach would require the boards path to get bigger, meaning more cells have to be rebuilt each timestep. Comparatively, the overset meshing would interpolate over the same number of cells (for the same mesh size)

regardless of fume cupboard width.

A mass flow rate boundary condition was placed on the outlet at 0.490 kg/s and a zero gradient pressure difference was applied to the inlets of the domain. All other boundaries are considered as no-slip walls.

Initially the flow was quiescent everywhere, and the flow was given five seconds to stabilise before the board motion began. The five second delay was trialled and found to be sufficient for the velocity field to become steady for this design of fume cupboard.

The motion of the board was defined using an expression function which stated that when the time is between 5 s and 7.7 s, the board moves at 1 m/s across the front of the fume cupboard, otherwise it is stationary.

It is worth noting that the current type test [1] has the board pass from one side to the other, then back after a 30 s pause between. The 30 s pause is sufficient for the velocity field to return to its original state. This means that, for symmetrical cupboards, the velocity field at the right hand side of the fume cupboard when the board passes left to right is the same as the left hand side when the board passes right to left and vice versa. This is shown in Fig. 7 where the peaks and troughs seen every 30 s are reversed at the left and right hand sides.

The same simulation was repeated with an outlet condition of

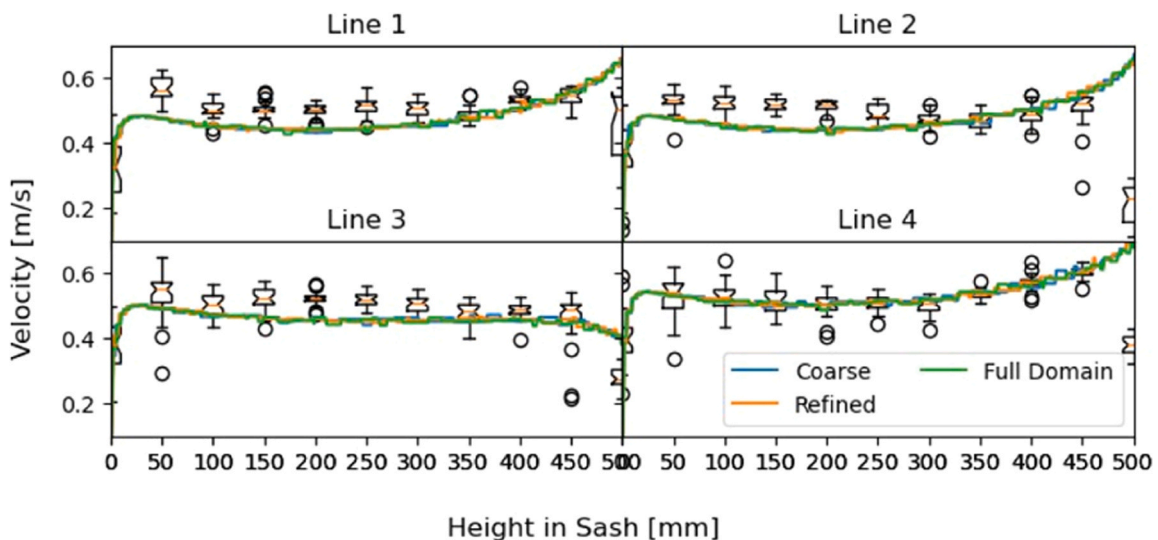


Fig. 8. Compar son of face ve oc ty at 0.5 m/s.

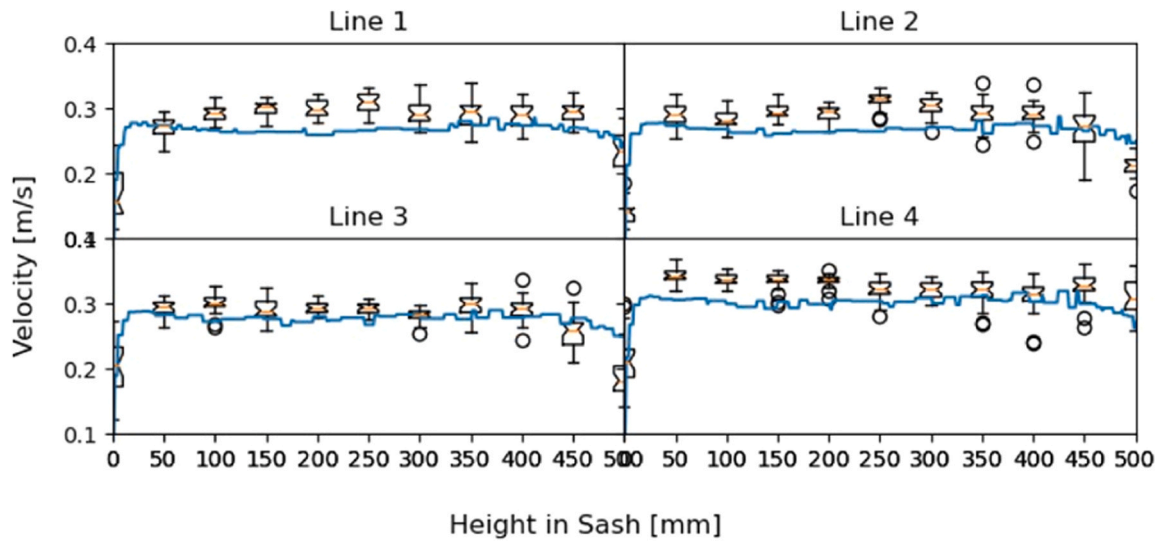


Fig. 9. Comparison of face velocity at 0.3 m/s.

Table 1  
MAPE during the static domain test.

Line No.	0.3 m/s	0.5 m/s
Line 1	4.14%	7.68%
Line 2	2.09%	2.90%
Line 3	1.20%	5.17%
Line 4	4.37%	3.96%

0.294 kg/s to give a face velocity of 0.3 m/s. Both simulations were identical in all other regards.

#### 4. Results & discussion

In this section, we report and analyse the velocity fields measured from experiments, described in Section 2, and compare them to those calculated using CFD simulations described in Section 3.

##### 4.1. Static domain

The velocity profile along lines 1–4 in the static domain was compared, as shown in Fig. 1. In the experiment, the velocity was measured at 50 mm intervals vertically along the 500 mm sash opening. Figs. 9 and 8 show the comparison of the 4 lines at 0.3 m/s and 0.5 m/s respectively and includes mesh independence results.

A full domain, which considered both halves of the fume cupboard instead of the symmetry plane, was compared to a coarse mesh and refined mesh which modelled a half domain, shown in Fig. 8. When the half domain was used a symmetry plane was placed at the centre of the fume cupboard, no numerical or air flow instability was noted using this approach.

It can be seen that a good agreement between experimental and simulated results is achieved at both face velocities and along each line. The results presented were taken after 15 s, which corresponds to around three residence times. During analysis, it was found that one residence time would have been sufficient for the velocity to stabilise.

The experimental results in Figs. 8 and 9 are presented in a traditional box plot format identifying the mean, inter quartile results and the range of the measured velocity at each height along Lines 1–4.

The Mean Absolute Percentage Error (MAPE) was used to compare the simulated and experimental results. The average percentage error at 0.5 m/s face velocity was 4.93% and 2.95% at 0.3 m/s. In both cases, the MAPE value was lower than the range of experimental

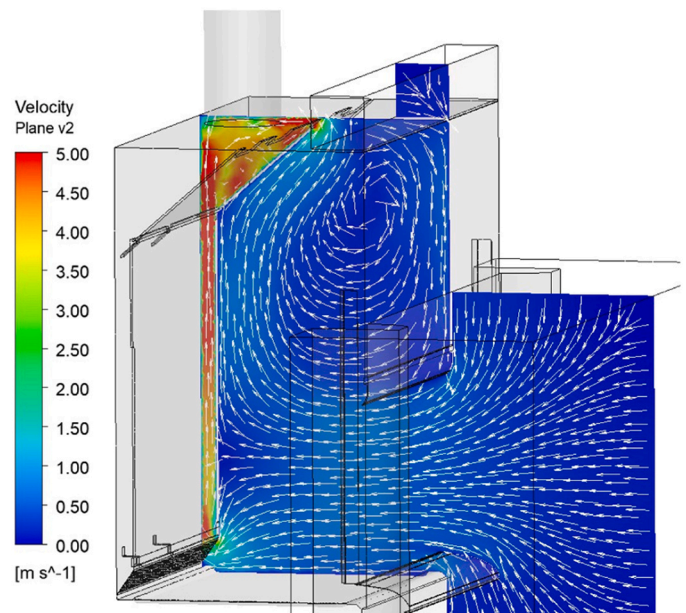


Fig. 10. Typical flow structure formed inside the fume cupboard.

measurements. The MAPE values for each line are presented in Table 1. Based on the MAPE being lower than the range of experimental values, and the trend being followed by the simulated results, it is clear that the simulations can produce a suitable alternative for testing a static domain.

The velocity field inside the fume cupboard is shown in Fig. 10 and is in keeping with expected trends seen in smoke visualisation conducted prior to experimental testing.

In the main chamber inside the fume cupboard, the air flow forms two paths. Below the sash handle, where operators regularly work, the air enters straight forward and clears the work surface, minimising the chance for any gas to escape. Above the sash handle, a recirculation zone is created, shown by Fig. 10. This has been regularly observed in experimentation and so is in keeping with the physics. This recirculation zone is inherent to the fume cupboard design and helps prevent fumes building up behind the sash.

The results also show that around 50% of the air passes beneath the baffle, the remainder splits over the baffle and beside the baffle evenly.



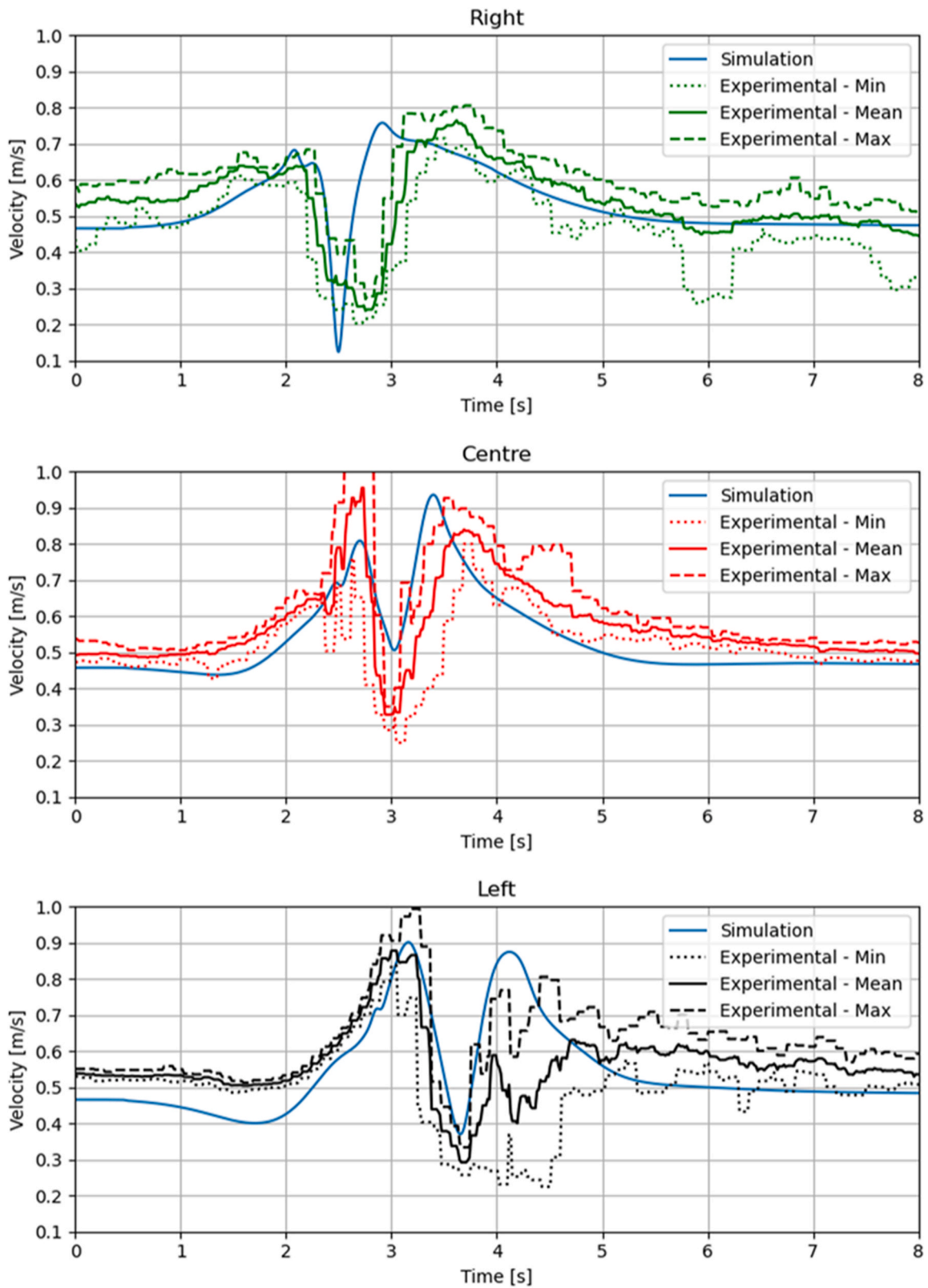


Fig. 11. Comparison of velocity in a dynamic domain with a face velocity of 0.5 m/s.

This matches with results taken during the experiment setup.

#### 4.2. Dynamic domain

The results from the dynamic mesh are shown in Fig. 11 and a good

agreement can be seen. The experimental

results show the maximum, minimum and mean values of the 5 experimental tests, and for the most part, the simulated values fit between the range.

The profile of the velocity graph is as expected. In the centre,

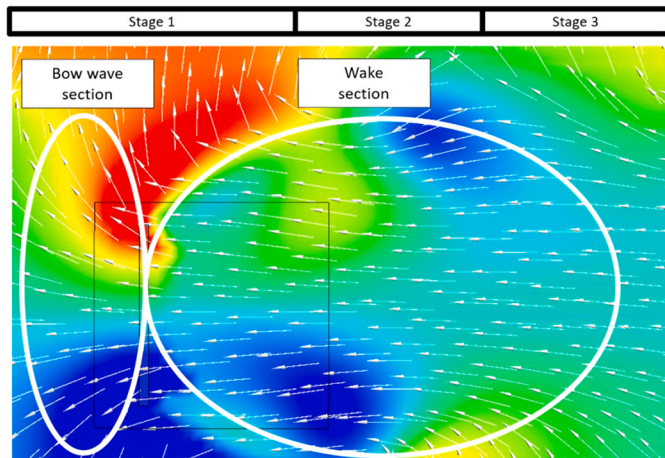


Fig. 12. X component of velocity around a moving board.

experiments show a maximum mean velocity of 0.9 m/s whereas only 0.8 m/s was simulated. This difference can partially be attributed to the unplanned board movement. In CFD, the board remains rigid throughout the movement. In practice, the board has a whipping effect where the board is fixed at the base and the top swings forwards and backwards as it moves. This movement is caused by the thickness of the board being just 20 mm and the height being 1.9 m. The board's stiffness was low, thus an additional level of movement was introduced which increased the face velocity in the experiments.

It is also possible to see that as the board moves from right to left, the simulation follows the experimental results. The right hand side is first affected, then the centre, then the left hand side. The shape of the velocity profile, shown in Fig. 11, is in keeping with the physics of the problem being modelled. Fig. 12 shows that the x-component of velocity around the board as it moves in front of the fume cupboard. In this figure, it is possible to see the bow wave and the wake region and Stages 1–3 of the board - fume cupboard interaction.

Consider a single point in the centre of the sash with the board passing in front. During stage 1, the velocity will increase as the bow wave 'pushes' air into the fume cupboard. This is minimised on the right hand side of the fume cupboard, shown in Fig. 11, because the side panel shields the right hand side. On the left hand side, the first peak is largest because the bow wave is unobstructed and has the longest time to develop.

During Stage 2, the wake generates a turbulent structure which causes a drop in velocity of between 20–50% and can draw air out of the fume cupboard. This is more prominent on the left hand side than in the centre because the turbulent structure has had more time to develop. At the right hand side, the turbulent structure interacts with the side panel

and the effect is amplified.

In the final stage, the face velocity increases again as the turbulent structure finishes, then the velocity tails off to its normal value.

The same simulation was conducted with a face velocity of 0.3 m/s and a summary of the results are shown below in Fig. 13. It can be seen in Fig. 13 that at 0.3 m/s face velocity, there remains a good agreement, demonstrating accuracy across the range of typical face velocities, 0.3–0.5 m/s.

During the dynamic the face velocity can drop to just 0.1/s, which is known to cause a drop in containment. The reason for this phenomena is shown graphically by Fig. 14 where the x-component drops to low levels.

This low x-velocity will sweep across the face of the fume cupboard with the boards wake. This effect will be lower on the side where the board starts, since the side panel of the fume cupboard will shield the region from the wake.

Whilst the impact of this low x-velocity was not assessed as part of this study, it is clear that the accurate modelling is essential for a future testing method to be viable.

### 5. Conclusion

The velocity field around a fume cupboard was modelled using a static and dynamic domain. The face velocity, which is a key factor in containing fumes within the chamber, was assessed throughout the study. During the present work, a mesh refinement trial and comparison of turbulence models were conducted ahead of the results being published.

The static domain was able to accurately show the velocity profile at the face of the fume cupboard. It was also able to capture the typical flow pattern around a fume cupboard which is in keeping with the physics of the problem.

It was also shown in Fig. 8 that the use of a half domain provides nearly identical results to a fully modelled simulation when a symmetry plane is correctly implemented. This provides a notable time

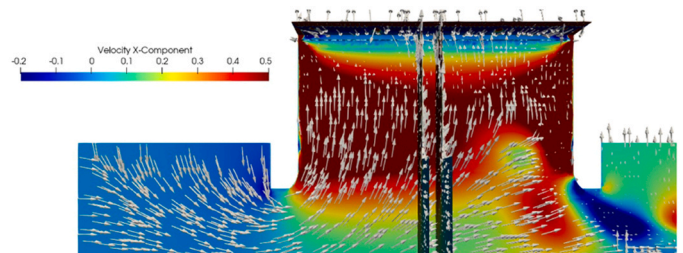


Fig. 14. A visualization of velocity fields which enable contaminants to escape. Figure is taken from above a fume cupboard looking down at the worktop.

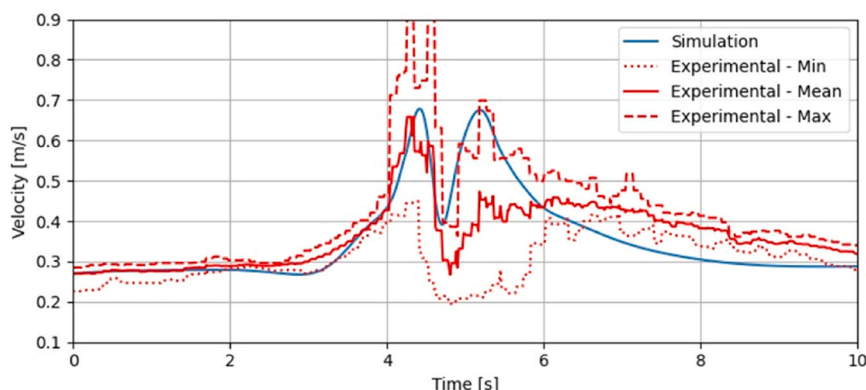


Fig. 13. Comparison of x velocity in a dynamic domain with a face velocity of 0.3 m/s.

advantage for this simulation approach.

In a dynamic domain, an overset meshing approach was used and the simulated values are in keeping with the experimental results. The results show that the simulations provided a reasonable agreement with the experimental measurements, and that the velocity field adjusts accurately with the board movement.

This means that CFD is capable of simulating the required dynamic domain problem with an acceptable level of accuracy. In turn, this means that a CFD based testing method is achievable.

In order for CFD to become an appropriate testing method for fume cupboards in the future, a suitable methodology must be developed. This testing method should maximise the capabilities of CFD, meaning it should assess the performance across the entire domain, rather than at specific locations used in the current methods which require injectors and measurement probes.

In addition, a new test method must provide standardised and client focused set of results. This will mean the client can understand clearly what is being tested at each stage, and can readily understand the results.

### Declaration of Competing Interest

The authors declare that they have no known competing financial interests or personal relationships that could have appeared to influence the work reported in this paper.

### Data Availability

The authors do not have permission to share data.

### Acknowledgements

The authors are grateful to Innovate UK for the funding of this KTP partnership (No. 1026924) and to Clean Air Ltd. for the use of their test facilities, support of the project and commitment to environmental sustainability.

### References

- [1] British Standards Institute. Fume cupboards - type test methods, 2019.
- [2] British Standards Institute. Fume cupboards - part 4: On-site test methods. 14175, 2004.
- [3] ISM Deutschland GmbH. S6 lasercheck p3:fh, 2022.
- [4] UNFCC. Global warming potentials (ipcc second assessment report) | unfccc, 2022.
- [5] Lord Rooker and Hilary Benn. Climate change act, 11 2008.
- [6] Kwangseog Ahn, Susan Woskie, Louis Diberardinis, Michael Ellenbecker, A review of published quantitative experimental studies on factors affecting laboratory fume hood performance, *J. Occup. Environ. Hyg.* 5 (2008) 735–753.
- [7] G.P. Nicholson, R.P. Clark, M.L. de Calcina-Goff, Computational fluid dynamics as a method for assessing fume cupboard performance, *Ann. Occup. Hyg. TA - TT - 44* (2000) 203–217.
- [8] Graham P. Nicholson, Raymond P. Clark, Fred Grover, A simple method for fume cupboard performance assessment, *Br. Occup. Hyg. Soc.* 44 (2000) 291–300.
- [9] P.J. Witt, C.B. Solnordal, L.J. Mittoni, S. Finn, J. Pluta, Optimising the design of fume extraction hoods using a combination of engineering and cfd modelling, *Appl. Math. Model.* 30 (2006) 1167–1179.
- [10] Ming Jyh Chern, Wei Ying Cheng, Numerical investigation of turbulent diffusion in push-pull and exhaust fume cupboards, *Ann. Occup. Hyg.* 51 (517–531) (2007) 8.
- [11] S.Jawomir Pietrowicz, Piotr Kolasiński, Michał. Pomorski, Experimental and numerical flow analysis and design optimization of a fume hood using the cfd method, *Chem. Eng. Res. Des.* 132 (2018) 627–643.
- [12] TSI Inc. Air velocity transducers models 8455, 8465, and 8475, 2012.
- [13] Clean Air Ltd. Radius profile fume cupboards - excellent containment - clean air, 2022.
- [14] Robert W. Fox, Philip J. Pritchard, Alan T. McDonald. *Introduction to Fluid Mechanics*, seventh ed., John Wiley & Sons, Ltd, 2010.
- [15] H.K. Versteeg and W. Malaskekerana *An Introduction to Computational Fluid Dynamics*, volume M. 2007.
- [16] Julius Oscar Hinze, *Turbulence*, second ed., McGraw-Hill, 1975.
- [17] William M. Chan. Overset grid technology development at nasa ames research center, 3 2009.
- [18] Hao Chen, Ling Qian, Zhihua Ma, Wei Bai, Ye Li, Derek Causon, Clive Mingham, Application of an overset mesh based numerical wave tank for modelling realistic free-surface hydrodynamic problems, *Ocean Eng.* 176 (97–117) (2019) 3.
- [19] Aidan Bharath, Irene Penesis, Jean-Roch Nader, and Gregor Macfarlane. Non-linear cfd modelling of a submerged sphere wave energy converter. *Asian Wave and Tidal Energy Conference*, 2016.
- [20] Domenico P. Coiro, Giancarlo Troise, Giuseppe Calise, Nadia Bizzarrini, Wave energy conversion through a point pivoted absorber: numerical and experimental tests on a scaled model, *Renew. Energy* 87 (317–325) (2016) 3.
- [21] James Allen, Konstantinos Sampanis, Jian Wan, Jon Miles, Deborah Greaves, and Gregorio Iglesias. Laboratory tests and numerical modelling in the development of wavecat. *Twelfth European Wave and Tidal Energy Conference*, 2017.
- [22] Ahmed Elhanafi, Gregor Macfarlane, Alan Fleming, Zhi Leong, Experimental and numerical investigations on the hydrodynamic performance of a floating-moored oscillating water column wave energy converter. *Appl. Energy* 205 (2017) 369–390.
- [23] Z. Lin, L. Qian, W. Bai, A coupled overset CFD and mooring line model for floating wind turbine hydrodynamics, *31st Int. Ocean Polar Eng. Conf.* (2021).
- [24] T. Erfani, H. Mokhtar, R. Erfani, Self-adaptive agent modelling of wind farm for energy capture optimisation, *Energy Syst.* 9 (2018) 209–222.
- [25] Christian Windt, Josh Davidson, John V. Ringwood, High-fidelity numerical modelling of ocean wave energy systems: a review of computational fluid dynamics-based numerical wave tanks, *Renew. Sustain. Energy Rev.* 10 (2018).
- [26] T. Erfani, R. Erfani, An evolutionary approach to solve a system of multiple interrelated agent problems, *Appl. Soft Comput.* 37 (2015) 40–47.
- [27] C. Hale, R. Erfani, K. Kontis, Multiple encapsulated electrode plasma actuators to influence the induced velocity: Further configurations., *40th Fluid Dynamics Conference and Exhibit*, (2010) 5106.